Phase separation of a polymer blend driven by oscillating particles

Yue-jin Zhu and Yu-qiang Ma*
National Laboratory of Solid State Microstructures, Nanjing University, Nanjing 210093, China
(Received 21 November 2002; published 23 April 2003)

We study the possible formation of ordered structures of a binary polymer blend by introducing mobile particles in a periodically oscillating driving field. The particles which have a preferential attraction to one of the immiscible phases, will significantly perturb the phase separation of the system and breakup the isotropy of the system, so that some interesting structures such as lamellar and cylinder phases are observed by appropriate selection of the simulation parameters. We examine in detail the dependence of formed morphology and domain size on the oscillating fields, the relative composition of mixtures, the diffusion coefficient, and quench depth, and then discuss how to realize stable and highly ordered structures.

DOI: 10.1103/PhysRevE.67.041503 PACS number(s): 64.75.+g, 83.10.Tv, 81.05.Zx

I. INTRODUCTION

The phase separation in a binary immiscible polymer mixture has been studied extensively theoretically and experimentally [1]. When the system is suddenly quenched below the spinodal line, the domain morphology may be an interconnected bicontinuous phase or isolated droplets, depending on the relative fraction of the two phases, and changes continuously in space and time. In order to obtain new and useful ordering structures due to its potential importance in the material engineering, some previous studies have considered the application of external perturbations (e.g., shear flows, electric field, temperature inhomogeneity, and surfaces) to control the domain curvature and orientation [2–10]. For example, depending on the frequency and amplitude of the oscillatory shear flow, the domain morphologies of the block copolymer system could be the lamellar structures either parallel or perpendicular to the flow direction [9–12].

Actually, the ordered structures can also be generated by means of the introduction of mobile particles to polymer blends [13–19]. In many technological applications, the use of colloidal or glass particles is a promising route to materials synthesis with the opportunity to create highly ordered structures on wide length scales. However, when the mobile particles are introduced, the growth dynamics may be changed due to the interplay of several dynamic mechanisms. Tanaka *et al.* [13] first provided experimental study on the pattern evolution in a binary mixture into which mobile particles were introduced with different interactions to two immiscible phases, and found that the presence of mobile particles dramatically changes the morphology and growth kinetics of the phase-separation. This phenomenon originates from the strong preferential attraction of the filler particles by one component of the blend. As we know, the presence of such a selective interaction will strongly affect the structure evolution and growth dynamics by competing with phase-separation process [13–16]. By combining cell dynamical systems (CDS) and Langevin dynamics for particles, Ginzburg *et al.* [17] studied the phase separation in a binary mixture for low particle density with selective affinity of one of the species. It was found that the addition of hard particles greatly changes both the speed and the morphology of the phase separation. However, in these studies, phase separation still led to an isotropic, disordered morphology of the coexisting phases. By using CDS method, we have studied the structure formation on the solid substrate of phase-separating films containing mobile particles with a preferential attraction for one component of the mixtures. It was shown that the presence of mobile particles under the surface-particle interaction modulation breaks the isotropy of the bulk phase-separating process, leading to the formation of orientational structures under a modulated pinning potential [18]. Recently, we have further reported the formation of striped patterns of a binary polymer film through periodic oscillatory particles with special addictive to one of the two immiscible phases. We observe the striped domain structures either parallel or perpendicular to the oscillatory direction by changing the oscillatory frequency and amplitude [20]. This indicates that the oscillatory particles can control the ordering morphology in phase separation of multicomponent mixtures.

In this paper, we study the formation of three-dimensional order structures of phase-separating systems by introducing mobile particles in a periodically oscillating field. The oscillatory external field enforces the movement of particles along oscillatory direction, and the particles in turn influence the phase-separating process due to an affinity for one of the components, resulting in the development of anisotropic structures. We find that the competition between the phase segregation and the deformation of the favored phase induced by mobile particles, can lead to continuous structures along the oscillation forcing direction and the lamellar structures perpendicular to the oscillatory direction. Depending on the strength of the oscillatory fields, we can observe highly ordered structures such as lamellar and cylindrical phases, contrary to the two-dimensional case. To discuss how to realize highly ordered lamellar structures, we have also investigated the dependence of the morphology and the domain size on the relative concentration between two phases, the diffusion coefficient, and quench depth.

The paper is organized as follows. Section II is devoted to the description of the model. In Sec. III, the numerical results

*Author to whom correspondence should be addressed. Electronic address: myqiang@nju.edu.cn

for pattern formation and growth behavior of phase separation are obtained and discussed. Finally, a brief summary is given in Sec. IV.

II. MODELS AND METHODS

We investigate a three-dimensional phase-separating system, and add a small concentration of particles subjected to periodically oscillating fields. We assume an externally alternating ''electric'' field acting on ''charged'' mobile particles along the x direction to describe the externally driving force. The local volume fractions of the components A, B and particles are denoted by $\phi_A(x,y,z)$, $\phi_B(x,y,z)$, and $\rho(x,y,z)$, respectively, and the total density $\phi_A(x,y,z)+\phi_B(x,y,z)+\rho(x,y,z)$ is assumed to be constant normalized to unity. Under the incompressibility condition, two of the local volume fractions will be independent. We take $\psi(x,y,z)=\phi_A(x,y,z)-\phi_B(x,y,z)$ and $\rho(x,y,z)$ as the independent variables. The order parameter $\psi(x,y,z)$ gives the local concentration difference between A ($\psi>0$) and B ($\psi<0$) phases, whereas the order parameter $\rho(x,y,z)$ describes the local particle concentration. We use a two-order-parameter model proposed by Komura *et al.* [21]. The free-energy function of the system is given by

$$F=\int\int\int dxdydz\left(-\frac{a}{2}\psi^2+\frac{b}{4}\psi^4+\frac{d}{2}(\nabla\psi)^2+e\rho^2(\rho-\rho_s)^2+g\rho\psi\right), \tag{1}$$

where parameters a, b, d, e, and g are positive constants. The e term allows the coexistence of two bulk states [21], i.e., $\rho=0$ and $\rho=\rho_s$. The state $\rho=0$ corresponds to the case in which the system is locally occupied either by A or B, whereas $\rho=\rho_s$ corresponds to the case in which the local volume is occupied only by the mobile particles. Here, we take into account a cross term g between the order parameters ψ and ρ due to the coupling between the mixture and the particles. $g>0$ means that the particle is energetically favorable in the B phase ($\psi<0$), and g is the interaction strength between the particles and the blend.

The dynamics of the phase-separating process is described by the coupled time-dependent Ginzburg-Landau equations [21–23] for the two order parameters ψ and ρ. We have [21]

$$\frac{\partial\psi}{\partial t}=M_\psi\nabla^2\frac{\delta F}{\delta\psi}, \tag{2}$$

$$\frac{\partial\rho}{\partial t}+\nabla\cdot\mathbf{j}_e=M_\rho\nabla^2\frac{\delta F}{\delta\rho}, \tag{3}$$

where M_ψ and M_ρ are mobility coefficients. The second term on the left-hand side of Eq. (3) comes from the addition current due to the existence of a driving field acting on particles. As is well known, the periodically oscillating field can be realized in many practical applications such as electrolytes, charged colloids, or granular materials. In the present work, a bias field is applied along the x axis, and the effect of driving the particles is analogous to that of an electric field on positive charges. This will cause the break down of symmetry in the system, and may significantly alter the macrophase separating structures. We neglect interactions between particles and consider only the particles' excluded volume constraint [24]. In the presence of oscillatory external field $\gamma\sin(\omega t)\hat{\mathbf{x}}$, pointing along unit vector $\hat{\mathbf{x}}$, a simple form of driving field can be modeled by the ''Ohmic'' current $\mathbf{j}_e=\gamma\sin(\omega t)\rho(1-\rho)\hat{\mathbf{x}}$ reflecting the vanishing of $\mathbf{j}_e$ in a completely filled or empty system [24]. Here, γ is the amplitude and ω is the frequency.

We perform numerical simulations of the model system using CDS approach by Oono and Puri [25,26]. The CDS equations corresponding to Eqs. (2) and (3) are written as

$$\begin{aligned}\psi(x,y,z,t+1)&=\psi(x,y,z,t)+M_\psi(\langle\langle I_\psi\rangle\rangle-I_\psi),\\ \rho(x,y,z,t+1)&=\rho(x,y,z,t)+M_\rho(\langle\langle I_\rho\rangle\rangle-I_\rho)\\ &\quad-\gamma\sin(\omega t)[1-2\rho(x,y,z,t)]\\ &\quad\times[\rho(x+1,y,z,t)-\rho(x-1,y,z,t)]/2,\end{aligned} \tag{4}$$

where

$$\begin{aligned}I_\psi&=-D(\langle\langle\psi\rangle\rangle-\psi)-A\tanh\psi+\psi+g\rho,\\ I_\rho&=E\rho(\rho-\rho_s)(2\rho-\rho_s)+g\psi,\end{aligned} \tag{5}$$

and

$$\langle\langle X\rangle\rangle=\frac{6}{80}\sum_{NN}X+\frac{3}{80}\sum_{NNN}X+\frac{1}{80}\sum_{NNNN}X, \tag{6}$$

where the subscripts NN, NNN, and NNNN stand for nearest-neighbor, next-nearest-neighbor, and next-next-nearest-neighbor cells, respectively. For the original cell dynamics system, the lattice size (Δx, Δy, or Δz) and the time step Δt were both set to be unity. The CDS parameters A, D, and E in Eq. (5) are related to the free-energy parameters in Eq. (1) by $A=1+a$, $D=d$, and $E=2e$ [27].

III. RESULTS AND DISCUSSION

Simulations are performed on a cubic $L\times L\times L=64\times 64\times 64$ lattice under periodic boundary conditions, and mobile particle phase 5%. The spatial averages of ψ and ρ are $\overline{\psi}=0$ and $\overline{\rho}=0.05$, respectively. We fix the parameters as $A=1.2$, $g=0.1$, $D=0.5$, $E=0.25$, $\rho_s=1$, and $M_\psi=M_\rho=0.05$. The effects of the strengths of driving fields on pattern selection are first investigated. The domain patterns for different parameters (a) $\gamma=0.02$, $\omega=0.002$ and (b) $\gamma=0.08$, $\omega=0.013$, are shown in Figs. 1 and 2, respectively. The gray color regions stand for A-rich domain, while light gray color regions represent B-rich domain. The particles are shown in black color. It can be clearly seen from Fig. 1 that for small oscillatory amplitude and frequency, the domain morphology displays a continuous structure along the oscil-

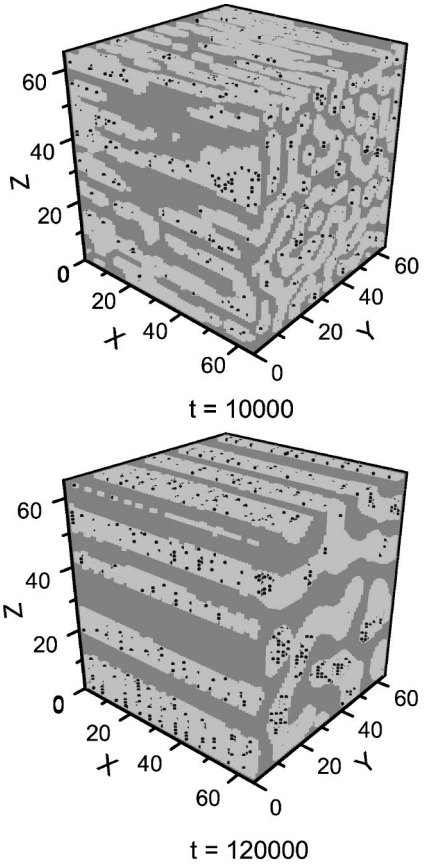

FIG. 1. Snapshot pictures of phase separation with $\gamma=0.02$, $\omega=0.002$, and $g=0.1$. Phase A is represented by the gray region, phase B by the light gray region, and the mobile particles by black.

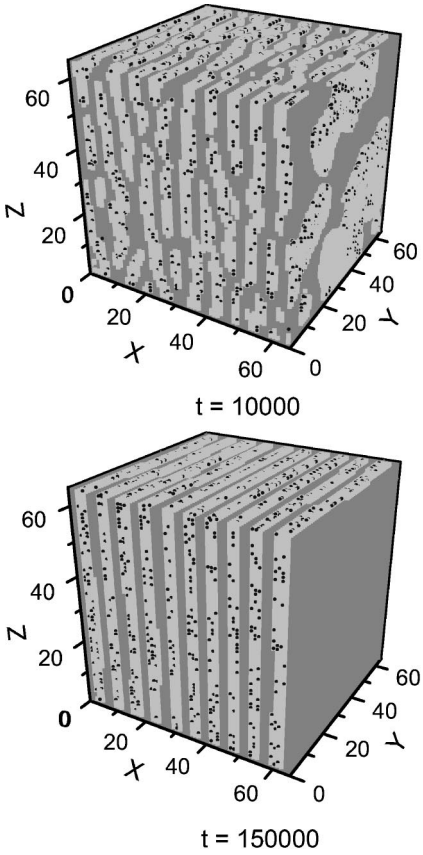

FIG. 2. Snapshot pictures of phase separation with $\gamma=0.08$, $\omega=0.013$, and $g=0.1$. Phase A is represented by the gray region, phase B by the light gray region, and the mobile particles by black.

latory forcing direction, i.e., the striped pattern is formed on the cross section parallel to the x axis (e.g., zx plane or xy plane). This may be due to the fact that the oscillatory motion of mobile particles will significantly breakup the symmetry of the system and enforce the coarsening process of the favored phase B adjusted to the motion of particles. The diffusion of B phase along the particle oscillatory direction is more strong than that of perpendicular direction. On the plane perpendicular to the x direction (yz plane), the isotropic macrophase separation is still not broken up. The particles are aggregated into the bulk phase B because this is energetically favorable. On the other hand, we observe from Fig. 2 that for large oscillatory amplitude and frequency, the particles drive the favored phase B to self-assemble into a lamellar structure which is perpendicular to the oscillatory direction. In fact, when the periodically oscillating force is strong enough, the favored phase B retains rapid motion along the oscillatory x direction due to sufficiently high oscillating frequency ω, while the movement of A component becomes relatively slow. On the other hand, due to the large amplitude γ, the moving range of the oscillatory particles is so large that the favored phase B is easily driven to extrude the A phase along the oscillatory direction, and thus the A phase is gradually crowded into thin domain perpendicular to the oscillatory direction. At the late stage, the thin domains A will join to form lamellar pieces perpendicular to the direction of the oscillatory force. Further, due to high frequency oscillation of the particle, its motion track can be effectively taken as a ''rodlike'' structure, and thus at the late stage, the structure and orientation of the system is seemly dominated by parallel ''rods,'' leading to the formation of smectic layer structures. As we know, such a lamellar pattern has been widely seen in smectic-A liquid crystal systems. In the present case, the oscillatory motion of particles suppresses the domain coarsening along the oscillatory direction, in contrast to the case observed in Fig. 1.

We can calculate numerically the domain size $R(t)$, which is derived from the inverse of the first moment of the structure factor $S(\mathbf{k},t)=\langle\psi_{\mathbf{k}}\psi_{-\mathbf{k}}\rangle$. For the x-axis continuous structure (Fig. 1), the domain morphology on the cross section (yz plane) is still isotropic structure. We introduce the mean characteristic size $R_{yz}(t)$ to describe the domain growth on yz plane

$$R_{yz}(t)=2\pi/\langle\overline{k}_{yz}(t)\rangle, \tag{7}$$

with

$$\langle\overline{k}_{yz}(t)\rangle=\sum_{i=1}^{L}\left[\int dkkS_i(k,t)\Big/\int dkS_i(k,t)\right]\Big/L, \tag{8}$$

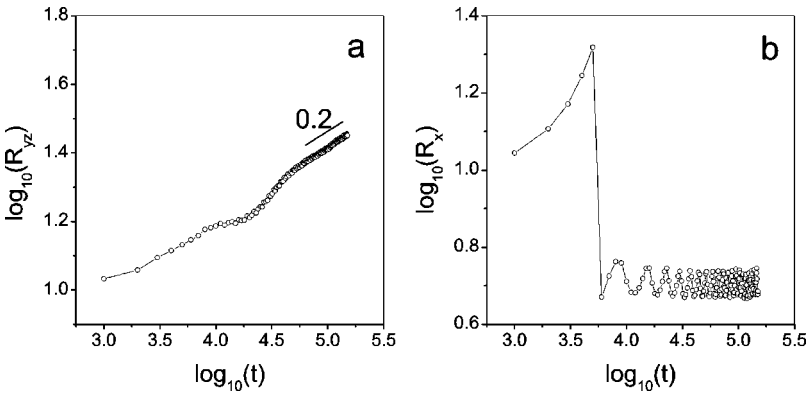

FIG. 3. Log-log plots of characteristic domain size vs time with (a) $\gamma=0.02$, $\omega=0.002$, $g=0.1$, and (b) $\gamma=0.08$, $\omega=0.013$, $g=0.1$.

where $S_i(k,t)$ is spherically averaged structure factor on yz plane with a fixed lattice index i at x axis, defined as $S_i(k,t)=\Sigma'_{k_y,kz}S(\mathbf{k},t)/\Sigma' 1$. On the other hand, for the lamellar structure shown in Fig. 2, the domain size R_x along the x direction which gives the thickness of lamella, is defined by $R_x=2\pi/\langle k_x(t)\rangle$, where $\langle k_x(t)\rangle=[\int d\mathbf{k}k_x^2 S(\mathbf{k},t)/\int d\mathbf{k}S(\mathbf{k},t)]^{1/2}$ [28,29]. All results are averaged over five independent runs. Figures 3(a) and 3(b) show the time evolution of the domain sizes R_{yz} and R_x for the parameters which are chosen to be the same as those in Figs. 1 and 2, respectively. We see from Fig. 3(a) that the growth exponent of the mean domain size $R_{yz}(t)$ is 0.2, which is evidently smaller than $\frac{1}{3}$ of Lifshitz-Slyozov (LS) coarsening mechanism [30]. This shows that the oscillatory motion of the particles slows down the process of phase separation on the yz plane perpendicular to the oscillatory direction, due to the pinning effect of the particles on the favored phase B [17,31]. On the other hand, it can be seen from Fig. 3(b) that for strong oscillatory force, the domain growth along x direction is quickly suppressed, and the characteristic domain size R_x is kept unchanged, approximately equal to 5.2 ± 0.4. We also see from Fig. 3(b) that at the late stage, a small periodic fluctuation in the characteristic domain size R_x is observed, due to the fact that the thin lamellar structure of B phase is easily affected by the enforced oscillation of the mobile particles, resulting in slight change of the lamellar width. Notice that in Fig. 3(b), as the time goes on, the growth curve R_x shows a sharp drop, signifying the morphology transition. At the early stage, the domain structure is disordered and R_x increases with time t. However, as the time is further increased, the system morphology changes from the disordered continuous to the lamellar structure. When this transition occurs, the domain size R_x drops to a lower value corresponding to the lamellar width. We should also point out that for weak oscillation case, because the continuous and parallel structure is formed along the oscillatory direction at the late stage, in principle, the x-direction domain size should be the lattice size. Therefore, in Fig. 3(a), we did not show the time dependence of the characteristic quantity R_x. Similarly, for strong oscillation case, due to the formation of parallel lamellar structures along yz plane, the domain size R_{yz} at the late stage is equal to the lattice size. In Fig. 3(b), we plot only R_x describing the lamellar width.

For weak oscillatory force, it will be interesting if we can realize the cylindrical structures along the oscillatory direction. Here, we discuss the effects of the variation of the relative composition of the two phases A and B on the formation of ordered cylindrical structures. By changing initial spatial average $\bar{\psi}$ for fixed $\gamma=0.02$ and $\omega=0.002$, Figs. 4(a), 4(b), and 4(c) show the changes of domain morphologies at $t=150\,000$ for (a) $\bar{\psi}=0.1$, (b) $\bar{\psi}=0.25$, and (c) $\bar{\psi}=0.4$, respectively. We see that with a gradual increase of the spatial average $\bar{\psi}$ (i.e., the B phase is decreased), the system still retains the x-direction continuous structure driven by the mobile particles under weak oscillatory force. On perpendicular yz plane, the oscillatory particles do not break the isotropic phase-separating process. Interestingly, as the concentration of the B-component is further decreased, the cylindrical structure may be formed. It is expected that the domain morphology on yz plane displays the circular droplets pattern, as seen from Fig. 5. Further, we can calculate the domain size of cylindrical structures, and easily see from Fig. 6 that the cylindrical structure is very stable due to the suppression of late-stage growth (the growth exponent is 0.01), contrary to those of high concentrations of B phase. This clearly indicates that in the present weak oscillating case, the stable cylindrical structures may be formed by changing the relative composition of polymer blends. Actually, the increase of $\bar{\psi}$ will breakup the composition symmetry of the system, namely, B phase becomes the minority one. Therefore, for a given particle number, the minority phase B is more easily disrupted by the oscillatory particles: on the one hand, the growth of domain is more seriously suppressed than that of the small $\bar{\psi}$ due to the particle-phase B coupling interaction; on the other hand, the circular domain on the yz plane is more easily formed for the minority phase B enclosed by the majority phase A due to the preferential attraction to B phase by oscillatory particles. If we perform the simulations of $\bar{\psi}>0.4$, the results also show the very stable cylindrical structures with the smaller sizes.

Furthermore, in order to discuss how to realize highly ordered lamellar structures under strong oscillating force, we investigate the dependence of the morphology and the domain size on the diffusion coefficient D and quench depths. We find that the competition between the phase segregation and the driven oscillating field acting on particles plays an important role on the formation of defect-free lamellar structures. Figure 7 displays the effects of effective diffusion coefficient D on the lamellar structures at time $t=150\,000$

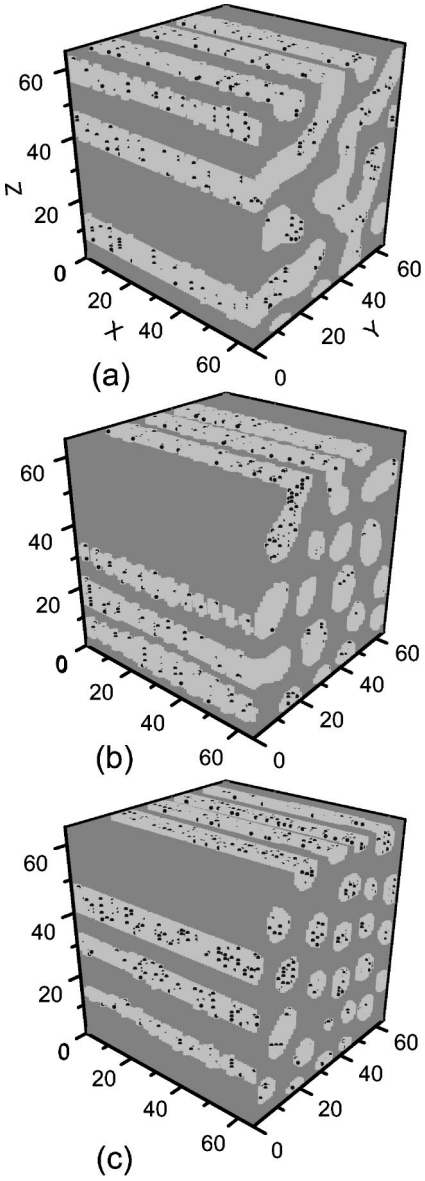

FIG. 4. Snapshot pictures of phase separation at $t=150\,000$ with $\gamma=0.02$, $\omega=0.002$, and $g=0.1$. (a) $\bar{\psi}=0.1$; (b) $\bar{\psi}=0.25$; (c) $\bar{\psi}=0.4$. Phase A is represented by the gray region, phase B by the light gray region, and the mobile particles by black.

when the oscillatory force is strong ($\gamma=0.08$ and $\omega=0.013$). We see that for lower value of the parameter D, there exist many topological defects such as disclinations. In this case, the phase separation of the system is too weak compared to the driven oscillating force acting on particles, so that the relatively strong disturbance on B phase due to the oscillatory motion of mobile particles produces some defects in lamellar structures. When the diffusion coefficient D is too large, some defects are still revealed due to very strong phase separation which largely lowers the oscillating effects. However, the effective diffusion coefficient D is hard to apparently affect on the domain size of formed lamellar structures. Figure 8 gives the time evolution of the lamellar thickness R_x for different diffusion coefficients D. The domain sizes are increased with the increase of D at the early stage, but

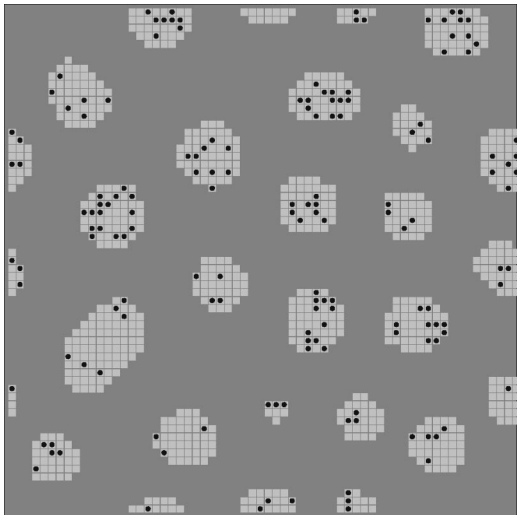

FIG. 5. Snapshot pictures of phase separation on yz plane (at the lattice index $i=64$ along x axis) with $\bar{\psi}=0.4$, $\gamma=0.02$, $\omega=0.002$, and $g=0.1$. Phase A is represented by the gray region, phase B by the light gray region, and the mobile particles by black.

their difference disappears gradually at the late stage.

Finally, we discuss kinetics of the formation of ordered lamellar phases for different quench depths. In Fig. 9, we show the pattern formation at $t=100\,000$ for fixed parameters $\gamma=0.08$ and $\omega=0.013$, by changing the temperature-dependent parameter $A=1+a$. We see that the topological defects of domain morphology increase with the increase of quench depth [i.e., larger A values such as $A=1.5$ in Fig. 9(b)]. As usual, as the quench deepens, domains easily form sharp interfaces and more defects may appear as a result of slow transport between clusters across interfaces. Therefore, the oscillation of particles may lose its role to remove topological defects, while the yz-plane lamellar structure remains. However, the quench depth has no appreciable effects on the lamellar domain width at late stage. Figure 10 shows the time evolution of the characteristic domain size R_x for

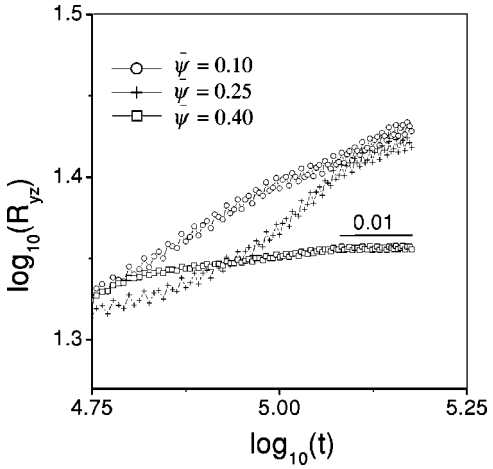

FIG. 6. Log-log plots of characteristic size R_{yz} vs time with $\gamma=0.02$, $\omega=0.002$, and $g=0.1$.

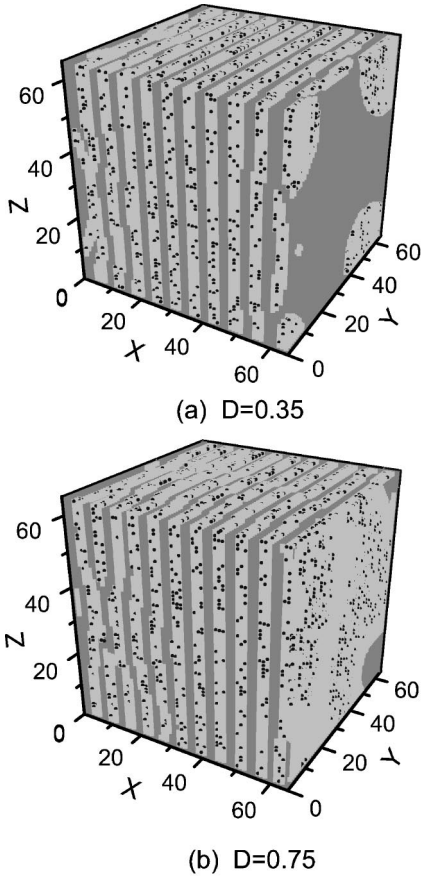

FIG. 7. Snapshot pictures of phase separation for different values of D at $t=150\,000$ with $\gamma=0.08$, $\omega=0.013$, and $g=0.1$. (a) $D=0.35$; (b) $D=0.75$. Phase A is represented by the gray region, phase B by the light gray region, and the mobile particles by black.

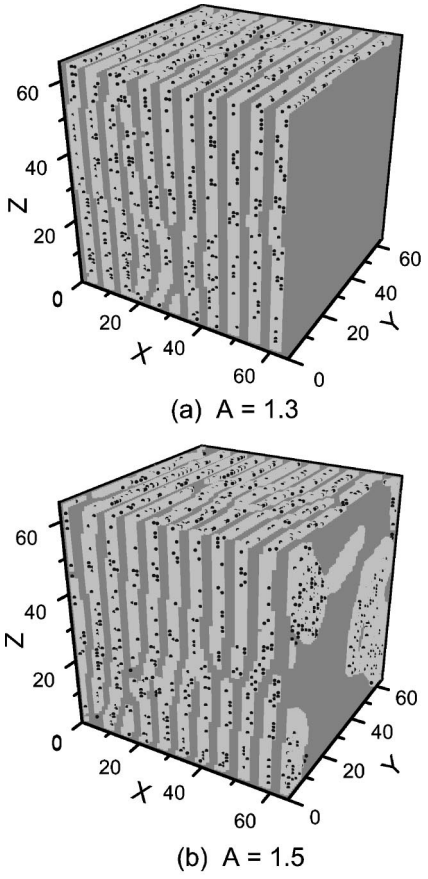

FIG. 9. Snapshot pictures of phase separation for deeper quenches at $t=100\,000$ with $\gamma=0.08$, $\omega=0.013$, and $g=0.1$. (a) $A=1.3$; (b) $A=1.5$. Phase A is represented by the gray region, phase B by the light gray region, and the mobile particles by black.

various values of the parameter A. The growth curves R_x show a sharp drop, signifying the morphology transition from the disordered continuous structure into the lamellar one. Especially, we can see clearly that the domain growth curves overlap at the late stage, i.e., the lamella width for different quench depths are of the same size. This indicates that the characteristic domain size of the lamellar structure is independent of the quench temperature, and is determined by only oscillatory frequency ω and amplitude γ under a fixed interaction strength g.

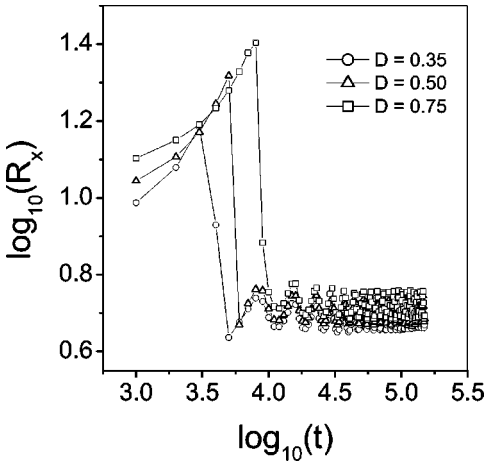

FIG. 8. Log-log plots of characteristic size R_x vs time with $\gamma=0.08$, $\omega=0.013$, and $g=0.1$.

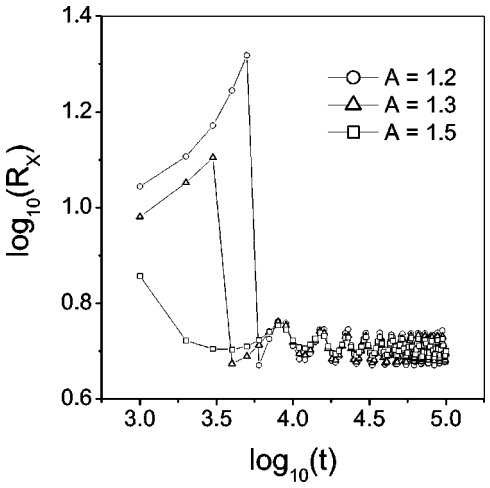

FIG. 10. Log-log plots of characteristic size R_x vs time with $\gamma=0.08$, $\omega=0.013$, and $g=0.1$.

IV. CONCLUSIONS

In this paper, we have studied the phase separation of a binary polymer blend with the inclusion of mobile particles under periodically oscillating driving fields, and examined the dependence of the morphology and the domain size on the oscillating fields, the relative composition between two phases, the diffusion coefficient, and quench temperature. The oscillatory particles breakup the isotropy of the system and anisotropically suppress composition fluctuations, leading to the formation of ordered structures by competing with the phase separation of the system. In particular, we observe a cylindrical phase parallel to the oscillatory direction under weak oscillating field and a defect-free lamellar phase perpendicular to the oscillatory direction under strong oscillating force. These highly ordered structures become very stable because the domain growths at the late stage are almost suppressed. We have also explored the effects of the diffusion coefficient and quench depth on the lamellar structures and corresponding growth dynamics, indicating that the defect-free lamellar structures may be realized by choosing reasonable parameters, and the characteristic thickness of the lamellar structure is mainly determined by the strength of oscillatory force acting on particles. Finally, we point out that for the overall electroneutrality constraint with zero total charge, we can consider a system with colloidal particles, each carrying positive or negative unit charge. A similar ordered pattern can be expected because the symmetry is also broken by an ''electric'' field which drives positive and negative charges in opposite directions. In addition, we can also introduce a short-ranged coupling interaction with Yukawa potential to describe the realistic case with ''counterions'' around charged particles. Further studies will be highly desirable.

ACKNOWLEDGMENTS

This work was supported by the China's Outstanding Young Foundation under Grant No. 19925415, the National Natural Science Foundation of China under Grant Nos. 90103035 and 10021001, and the Croucher Foundation of Hong Kong.

[1] J.D. Gunton, M. San Miguel, and P.S. Sahni, in *Phase Transitions and Critical Phenomena*, edited by C. Domb and J.L. Lebowitz (Academic, New York, 1983), Vol. 8; K. Binder, in *Phase Transitions in Materials*, edited by R.W. Chan, P. Haasen, and E.J. Kramer, *Materials Science and Technology* (VCH, Weinheim, 1990), Vol. 5; A.J. Bray, Adv. Phys. **43**, 357 (1994).
[2] F. Corberi, G. Gonnella, and A. Lamura, Phys. Rev. Lett. **83**, 4057 (1999).
[3] K. Krishnan, K. Almdal, W.R. Burghardt, T.P. Lodge, and F.S. Bates, Phys. Rev. Lett. **87**, 098301 (2001).
[4] C. Cutillas and G. Bossis, Europhys. Lett. **40**, 465 (1997).
[5] S. Zhu, Y. Liu, M.H. Rafailovich, J. Sokolov, D. Gersappe, D.A. Winesett, and H. Ade, Nature (London) **400**, 49 (1999).
[6] H. Tanaka and T. Sigehuzi, Phys. Rev. Lett. **75**, 874 (1995).
[7] T. Mullin, Phys. Rev. Lett. **84**, 4741 (2000).
[8] S.R. Ren, I.W. Hamley, P.I.C. Teixeira, and P.D. Olmsted, Phys. Rev. **63**, 041503 (2001).
[9] H. Leist, D. Maring, T. Turn-Aibrecht, and U. Wiesner, J. Chem. Phys. **110**, 8225 (1999).
[10] Z.R. Chen, J.A. Kornfield, S.D. Smith, J.T. Grothaus, and M.M. Satkowski, Science **277**, 1248 (1997).
[11] K. Koppi, M. Tirrell, F.S. Bates, K. Almdal, and R.H. Colby, J. Phys. II **2**, 1941 (1992).
[12] I.W. Hamley, J. Phys.: Condens. Matter **13**, R643 (2001).
[13] H. Tanaka, A.J. Lovinger, and D.D. Davis, Phys. Rev. Lett. **72**, 2581 (1994).
[14] H. Tanaka, Phys. Rev. Lett. **70**, 2770 (1993); S. Puri and K. Binder, J. Stat. Phys. **77**, 145 (1994); A. Budkowski, F. Scheffold, and J. Klein, J. Chem. Phys. **106**, 719 (1997); A. Karim, J.F. Douglas, B.P. Lee, S.C. Glotzer, J.A. Rogers, R.J. Jackman, E.J. Amis, and G.M. Whitesides, Phys. Rev. E **57**, R6273 (1998); A. Chakrabarti, J. Chem. Phys. **111**, 9418 (1999).
[15] P. Wiltzius and A. Cumming, Phys. Rev. Lett. **66**, 3000 (1991).
[16] M. Boltau, S. Walheim, J. Mlynek, G. Krausch, and U. Steiner, Nature (London) **391**, 877 (1998).
[17] V.V. Ginzburg, F. Qiu, M. Paniconi, G. Peng, D. Jasnow, and A.C. Balazs, Phys. Rev. Lett. **82**, 4026 (1999); V.V. Ginzburg, G. Peng, F. Qiu, D. Jasnow, and A.C. Balazs, Phys. Rev. E **60**, 4352 (1999).
[18] Y.Q. Ma, Phys. Rev. E **62**, 8207 (2000).
[19] Y.L. Tang and Y.Q. Ma, J. Chem. Phys. **116**, 7719 (2002).
[20] Y. J. Zhu and Y. Q. Ma, J. Chem. Phys. **117**, 10207 (2002).
[21] S. Komura and H. Kodama, Phys. Rev. E **55**, 1722 (1997).
[22] M. Laradji, H. Guo, M. Grant, and M.J. Zuckermann, J. Phys. A **24**, L629 (1991).
[23] A. Ito, Phys. Rev. E **58**, 6158 (1998).
[24] B. Schmittmann and R.K.P. Zia, Phys. Rep. **301**, 45 (1998); B. Schmittmann, Int. J. Mod. Phys. B **4**, 2269 (1990); B. Schmittmann and R.K.P. Zia, in *Phase Transitions and Critical Phenomena*, edited by C. Domb and J.L. Lebowitz (Academic, New York, 1995), Vol. 17.
[25] Y. Oono and S. Puri, Phys. Rev. Lett. **58**, 836 (1987); S. Puri and Y. Oono, Phys. Rev. A **38**, 1542 (1988).
[26] Y. Oono and S. Puri, Phys. Rev. A **38**, 434 (1987); A. Shinozaki and Y. Oono, *ibid.* **45**, 2161 (1992); A. Shinozaki and Y. Oono, Phys. Rev. E **48**, 2622 (1993).
[27] J.R. Roan and E.I. Shakhnovich, Phys. Rev. E **59**, 2109 (1999).
[28] E. Corberi, G. Gonnella, and A. Lamura, Phys. Rev. Lett. **83**, 4057 (1999); **81**, 3852 (1998).
[29] E. Corberi, G. Gonnella, and A. Lamura, Phys. Rev. E **61**, 6621 (2000).
[30] I.M. Lifshitz and V.V. Slyozov, J. Phys. Chem. Solids **19**, 35 (1961).
[31] K. Chen and Y.Q. Ma, Phys. Rev. E **65**, 041501 (2002).